Secondary Particle Showers from Hadron Absorber Interactions

Branton DeMoss
University of Colorado Boulder
High Energy Physics Group

May 10, 2016

Abstract

We simulate the contamination of muons from hadron absorber interactions in the current design of the LBNF beamline, which affects measurements relevant to accurately determining neutrino flux. Large scale ($\sim 10^7$ protons-on-target) GEANT4 simulations of the current beamline geometry show that up to 10% of low energy neutrinos at the near detector come from hadron absorber interaction events. These absorber-created neutrinos are detected at the far detector much less frequently, leading to new uncertainties in the expected ratio of near to far neutrino detection events. There is also an increased contamination of muon flux from absorber-created muons, adding additional background to muon monitoring efforts.

1 Introduction

The addition of new, complex geometry to the downstream hadron absorber in the LBNF beamline could present problems related to decays of secondary particles created in the absorber. Proton pulses from Fermilab's Main Injector interact with a solid graphite target to produce kaons and pions. Two focusing horns direct these products down the decay pipe aimed at the near and far detectors. Any particles that have not decayed by the end of the pipe are stopped via interaction with the hadron absorber. This technical note discusses the secondary effects of interactions with the hadron absorber, such as secondary showers that could potentially interfere with flux measurements, particularly neutrino and muon fluxes. In short, we'd like to assess how secondary particles created from hadron absorber interactions affect total particle production, and whether these secondary particles contribute significant error to flux measurements.

2 New Geometry

Recent [1] LBNF design documents have called for "scallops" to be placed in the absorber hall region. These are foot-thick aluminum blocks with spherical cuts taken out. Additionally, there is a proposal to add a foot thick solid block of aluminum to the front of the absorber region, the so-called "spoiler".

The spherical sculpts in the scallops have a radius of curvature of 0.35 meters, cut from the block such that the resultant thickness of the scallop along the beamline is 12.5 centimeters. Simulations were done with 200kA horn current and 120GeV proton energy.

Our first task was to implement the new geometry Fig. 2.1 into G4LBNE, a GEANT4 implementation of the LBNF experiment managed by Fermilab. The new geometry was implemented according mostly to [2] , with some supplementary information from Jan Boissevain's 3D model.

Most of the absorber hall region was remade to ease the implementation of the new geometry. In addition to the modifications to geometry construction source files, we created some new inputs to aid in muon and pion tracking. If our changes are added to the master branch of G4LBNE, the commands

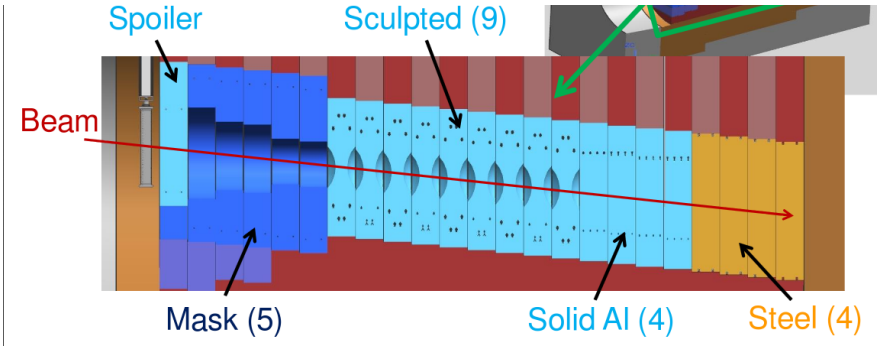

Figure 2.1: The current configuration of the absorber

```
/LBNE/output/doPionVertexTracking bool
/LBNE/output/doMuonVertexTracking bool
```

will add an output Ntuple to the results file with plenty of useful information.

3 Contamination Studies

Behind the absorber hall is the "Muon alcove", inside of which are various instruments to observe stopped and through-going muons, in order to correlate muon and neutrino flux data. Therefore, if muon production rates inside the absorber volumes significant, these absorber-born muons (which are generally poor proxies for neutrinos compared to muons created in the decay pipe) will make muon/neturino correlation more difficult. Of interest, then, is the percent of all forward going muons created in absorber volumes, and their momentum distribution.

3.1 Muon Distributions

As expected, the muon profile at the tracking plane downstream of the absorber is fairly tight. If, instead of plotting the complete Fig. 3.1a distribution, we cut muons by birth position and plot only those born in absorber volumes, we find the distribution of muons born in the hadron absorber has a similar spread.

Taking the ratio of the total muon profile Fig. 3.1b to the absorber muon profile Fig. 3.1c we see that the further from the center of the beam we get, the fewer absorber-created muons we find, relative to the primary muon beam spread. With further simulations of more particles, it should be straightforward to get a handle on exactly how the background muon flux from absorber interactions changes.

3.2 Muon counting methods

Our original method of counting muons used the detectors downstream of the absorber in the standard G4LBNE implementation. When a muon hits the detectors we get its birth position using the built-in

```
const G4ThreeVector& GetVertexPosition() const;
//See G4Track.hh for reference
```

then, we simply divide the number of muons born in absorber volumes by the total number of muons that hit the tracking plane. Using this method, we find that the muon contamination from absorber volumes is, depending on specific run settings, around 3% averaged across the entire plane in the new geometry, and up to about 10% at the beam center.

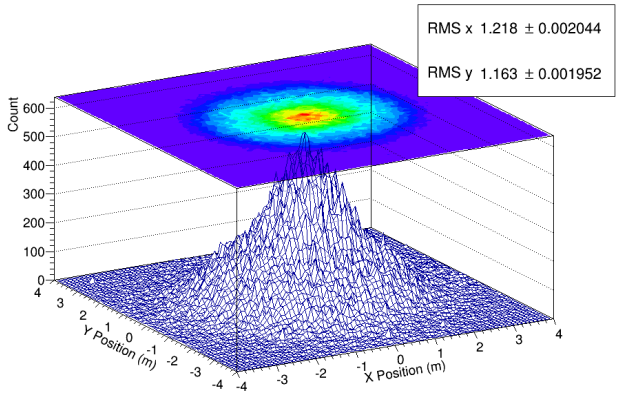

(a) Complete muon profile at tracking plane

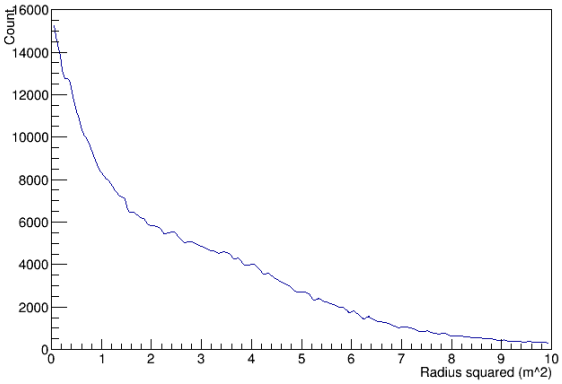

(b) Muon profile at tracking plane as a function of r^2

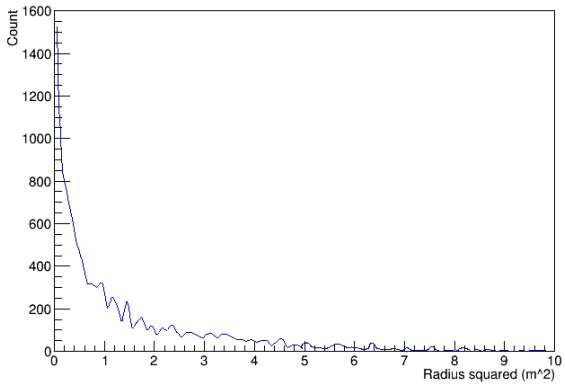

(c) Profile of absorber born muons

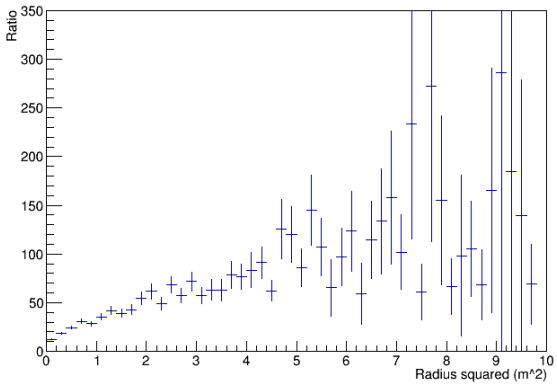

(d) Ratio of Fig. 3.1b to Fig. 3.1c

Figure 3.1: Muon profile distributions

As a check, we also used a double tracking-plane method to count muons. In this second method, we construct tracking planes both before and after the absorber hall, dividing the count of muons that hit only the back absorber by the total number that hit the back. This method gives numbers in agreement with our original method.

3.3 Weighted counts

Also of interest to our studies is the degree of pion contamination from the absorber region. Here we would like to introduce a different view of what constitutes an "important" particle. Because muons are directly measured in the Muon Alcove, how their production rates change matters, neutrino production notwithstanding. Pions, however, are not directly measured, so we only consider those which are "important" with regards to how they contribute to neutrino flux at the detectors. Figure 3.2 shows pion births weighted with their eventual contribution to neutrino flux at the near detector [1], which gives us an accurate picture of how pion contamination in the absorber affects neutrino production.

There is a clear spike in "important" pion births beginning at around 220 meters, which is the start of

[1] In reality we are counting neutrino events at the near detector and taking all those which come from pion decays. Then, we generate the pion importance graph with the parent pion's birth position, weighted by the neutrino's contribution to near detector flux.

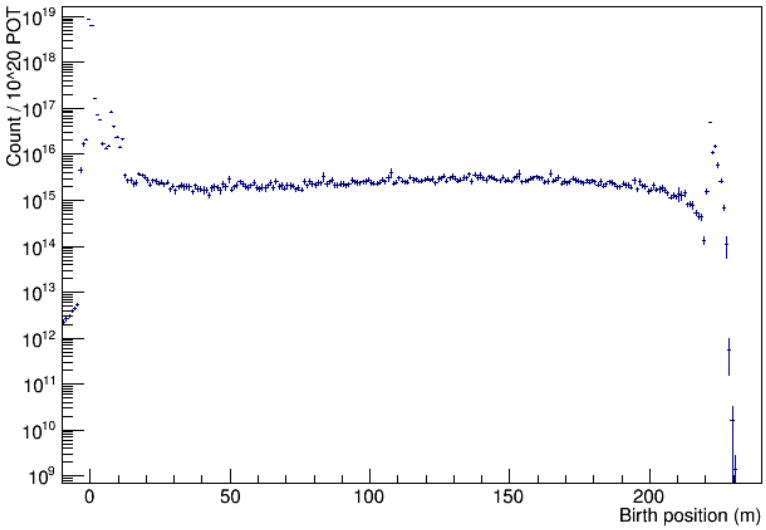

Figure 3.2: Pion births weighted with neutrino flux at near detector

the hadron absorber. Integrating this spike and dividing by the total pion count integral, we find that the percentage of "important" pion contamination from the hadron absorber is around 0.5%.

If we weight muon births by near detector neutrino flux, we find that there is not nearly as significant a spike at the absorber hall:

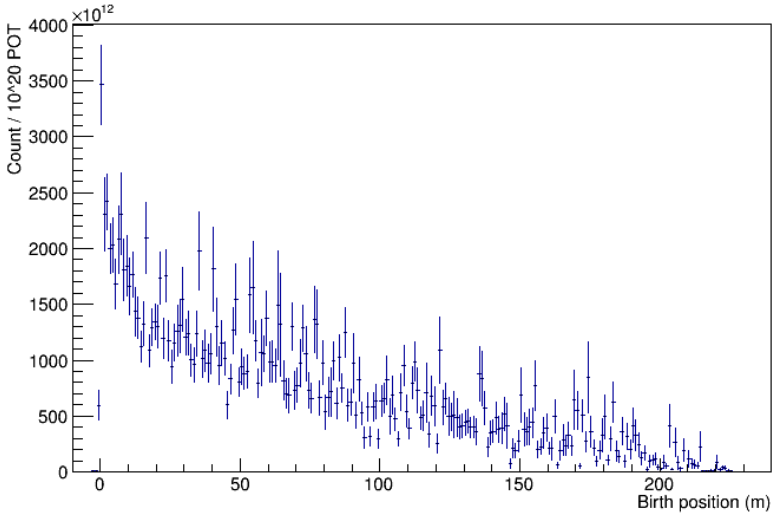

Figure 3.3: Muon births weighted with neutrino flux at near detector

Using the same pion contamination analysis as above, we find that the percentage of "important" muon contamination from the absorber regions is around 0.3%.

Note the difference in total muon contamination (which the Muon Alcove will measure) and the "important" muon contamination.

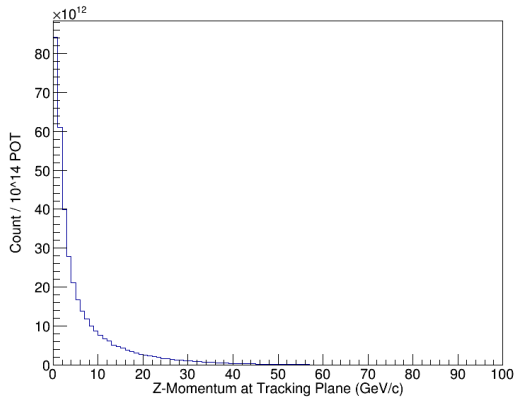

Figure 3.4: Pre-absorber muon momentum distribution

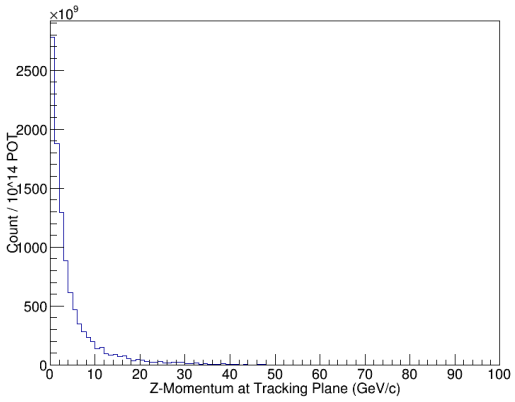

Figure 3.5: Absorber-born muon momentum distribution

Figs. 3.4 & 3.5: Momentum distributions at tracking plane

3.4 Momentum Distributions

Both the pre-absorber Fig. 3.4 and absorber-born Fig. 3.5 muons follow a steep drop off in z-momentum at the tracking plane after passing through absorber volumes.

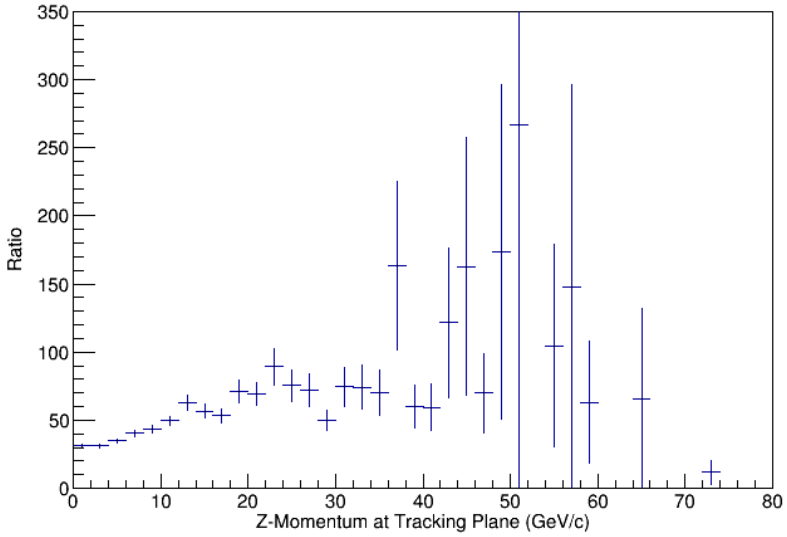

Figure 3.6: Ratio of pre-absorber to absorber muon momentum distributions

The momentum distribution ratio Fig. 3.6 shows that the fraction of absorber-created muons measured at any given momentum is less than 3%, often far less. This distribution is shown in Fig. 3.7 for an anti neutrino mode run.

Also of interest to our study is analyzing how the hadron absorber affects muon energy distributions.

Fig. 3.8 shows how the hadron absorber tends to decrease and smooth out the energy distribution of detected muons.

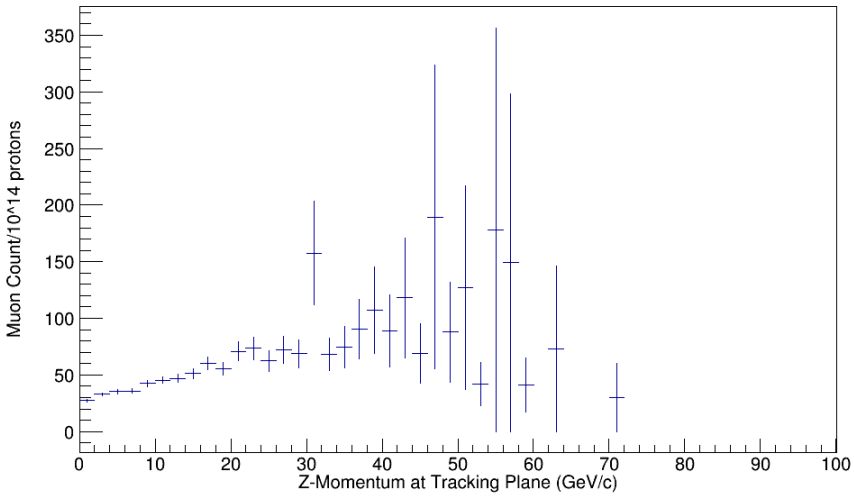

Figure 3.7: Ratio of pre-absorber to absorber muon momentum distributions in anti neutrino mode

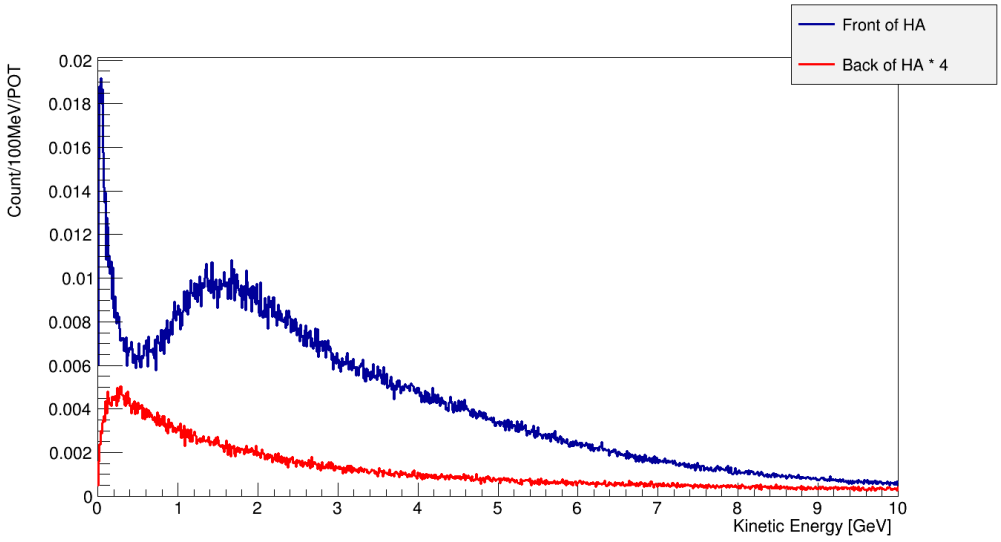

Figure 3.8: Muon energy distribution at front and back of absorber

4 Neutrino Flux

Of the utmost importance for this analysis is determining how neutrino flux changes with the addition of the hadron absorber. Especially, we would like to know if absorber-born neutrinos affect the near and far detection rates differently, and if so, by how much.

Our first graph Fig. 4.1 is a plot of the flux of various neutrino flavors. Comparison to similar plots [4] made for DUNE science documents shows that there are not severe differences with the new absorber geometry.

Looking into how specific neutrino detection rates change reveals that the ratio of near to far absorber-born counts does indeed change:

The contamination of absorber-born neutrinos at the near detector is more than double that of the far detector.

Neutrino Mode	ν_μ	$\overline{\nu_\mu}$	ν_e	$\overline{\nu_e}$
Near	0.33%	3.32%	0.91%	2.61%
Far	0.13%	1.26%	0.41%	1.03%

Table 1: Percentage of detector neutrino flux from absorber volume

Plotting the neutrino flux at the far detector, we see a similar flux distribution.

The overall flux at the near Fig. 4.1 and far Fig. 4.2 detectors are useful, but of greater relevance to this study is the percentage of flux of a given flavor from the absorber volumes, as a function of energy.

These plots Fig. 4.3 (found on last page) show how absorber-born neutrino count rates compare to the total neutrino count rate at the near and far detectors, as a function of energy. Here, then, are the most significant results of the study. At low energies (< 1 GeV) up to 10% of muon and anti-muon neutrinos detected come from absorber volumes (Fig. 4.3a and Fig. 4.3b).

4.1 Antineutrino mode

If we run our simulation with a negative current in the focusing horns, this is known as "antineutrino mode", as this will select the opposite sign particles for focusing, which will favor antineutrino production. The effects from the absorber are, as before:

Comparing Table 2 with Table 1 we see the expected favoring of the opposite sign, though with a notable increase in ν_e production in the absorber.

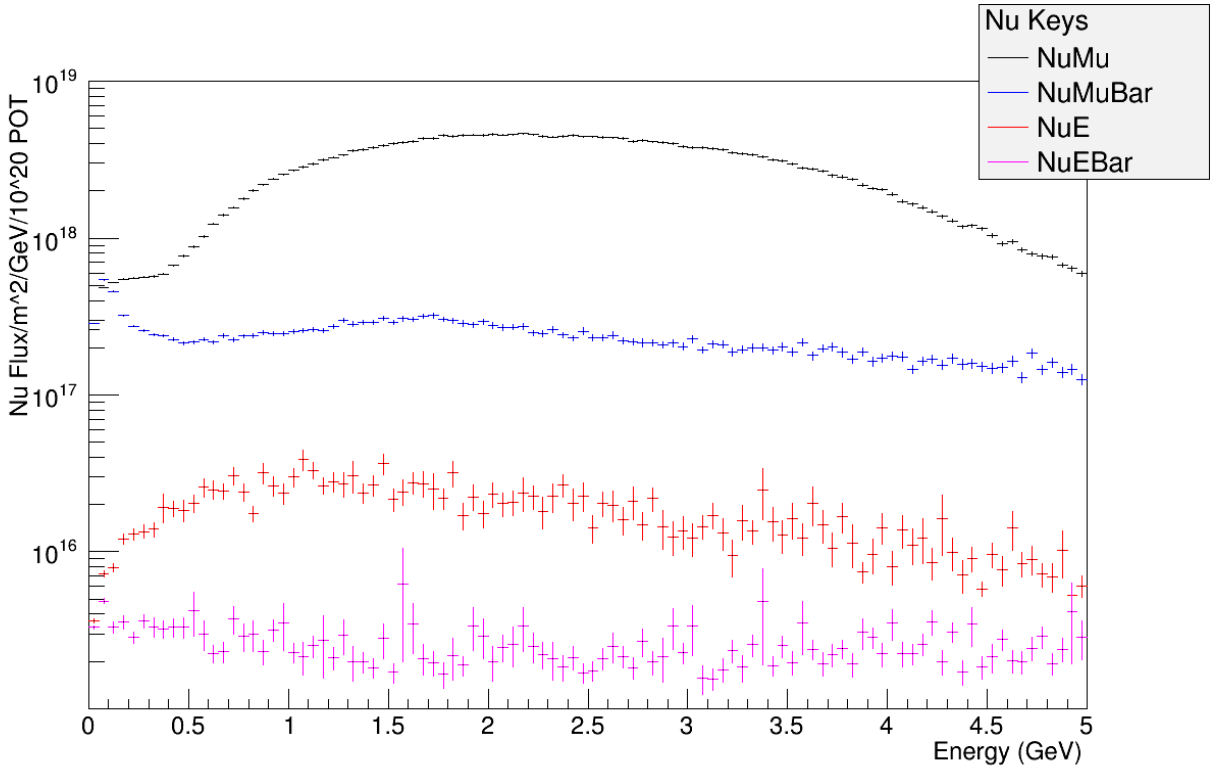

Figure 4.1: Neutrino flux of various flavors at the near detector.

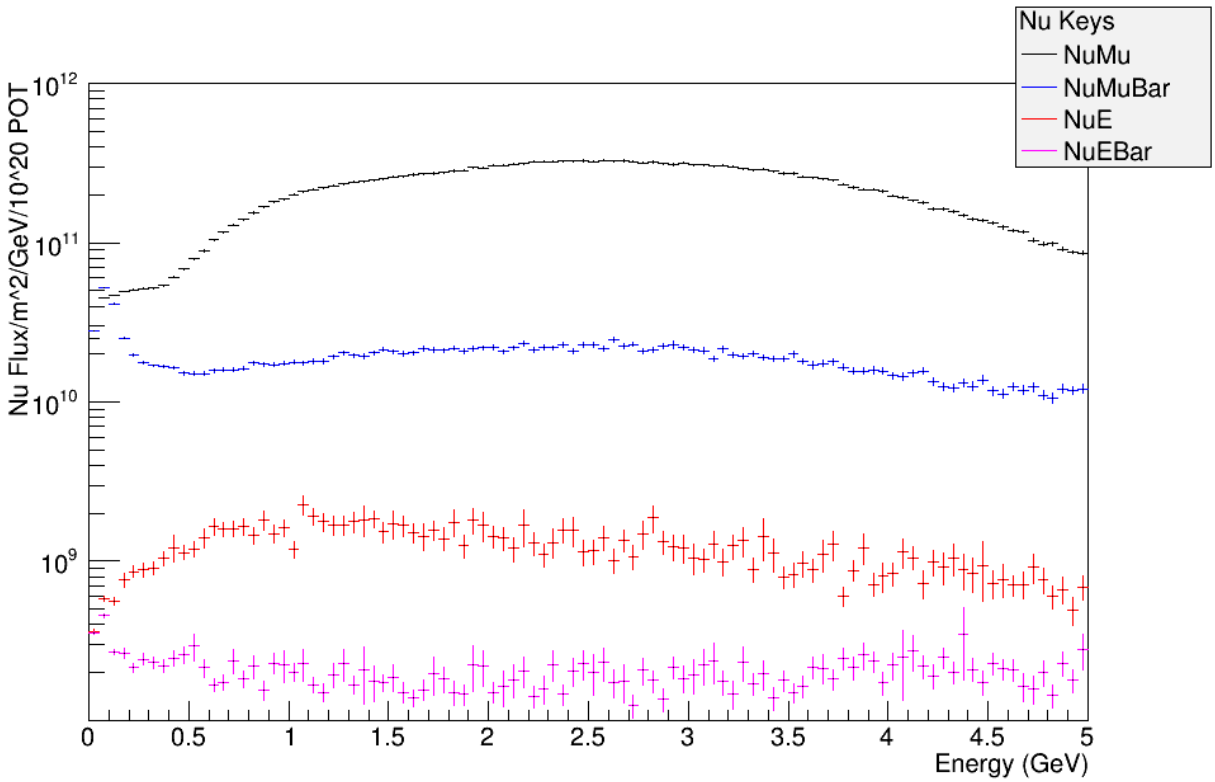

Figure 4.2: Neutrino flux of various flavors at the far detector.

Antineutrino Mode	ν_μ	$\overline{\nu_\mu}$	ν_e	$\overline{\nu_e}$
Near	3.47%	0.31%	4.13%	0.60%
Far	1.29%	0.12%	1.68%	0.27%

Table 2: Percentage of detector neutrino flux from absorber volumes (in antineutrino mode)

5 Conclusions

Absorber created neutrino contamination is an issue of varying magnitude at each detector, making near and far detector event correlation more error prone than originally anticipated. The ratio plots of neutrino flux from the absorber regions to total flux as a function of energy (Fig. 4.3) show how low energy neutrinos from the absorber make up around 10% of measured events at worst.

Absorber created muon contamination is also nontrivial. We show in Fig. 3.1d how the background of absorber-created muons changes with radius. This additional muon background will need to be taken into account to make accurate muon flux counts, when correlating muon and neutrino events.

This absorber design, with low-density materials and internal voids, results in non-trivial contamination of muons used for monitoring, and changes the neutrino near/far flux ratio by a significant amount.

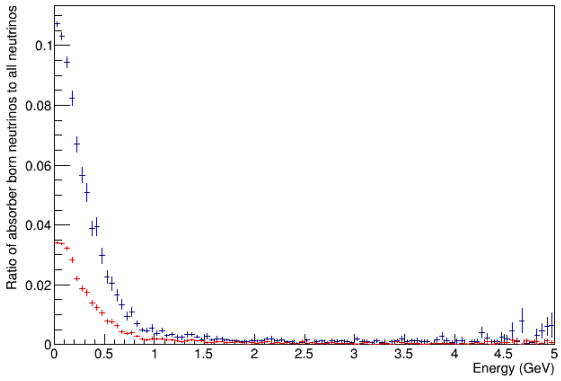

(a) Muon neutrinos

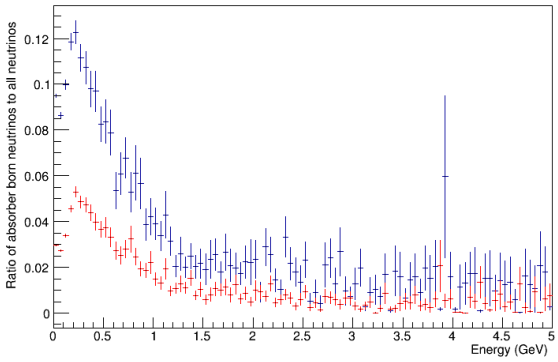

(b) Anti muon neutrinos

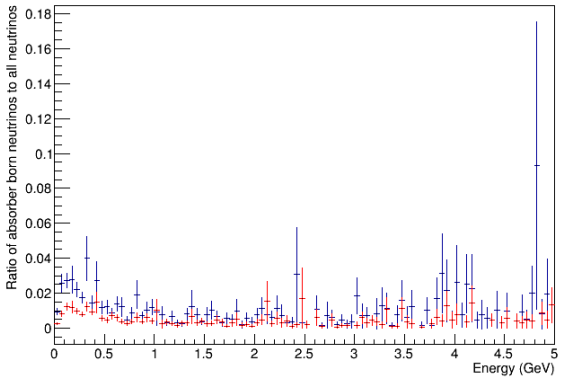

(c) Electron neutrinos

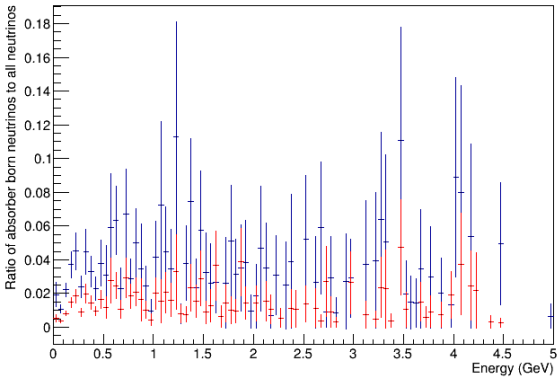

(d) Anti electron neutrinos

Figure 4.3: Ratio of absorber born to total neutrino flux at the detectors, graphed by flavor. Far detector in red. Running in neutrino mode.

References

[1] LBNE-doc-10092

[2] LBNE-doc-10095

[3] LBNE-doc-11203

[4] https://sharepoint.fnal.gov/project/lbne/LBNE at Work/science doc pdfs/chapter_3_optim.pdf (figure 3.18)